257

Copy
RM E52K14

RESEARCH MEMORANDUM

FORCE AND PRESSURE RECOVERY CHARACTERISTICS AT SUPERSONIC SPEEDS OF A CONICAL SPIKE INLET WITH BYPASSES DISCHARGING IN AN AXIAL DIRECTION

By J. L. Allen and Andrew Beke

Lewis Flight Propulsion Laboratory
Cleveland, Ohio

NATIONAL ADVISORY COMMITTEE
FOR AERONAUTICS
WASHINGTON
January 30, 1953

[redacted]

NATIONAL ADVISORY COMMITTEE FOR AERONAUTICS

RESEARCH MEMORANDUM

FORCE AND PRESSURE RECOVERY CHARACTERISTICS AT SUPERSONIC SPEEDS OF A CONICAL SPIKE INLET WITH BYPASSES DISCHARGING IN AN AXIAL DIRECTION

By J. L. Allen and Andrew Beke

SUMMARY

An axially symmetric nacelle-type conical spike inlet with two bypasses located in the horizontal plane and on opposite sides of the nacelle was investigated in the Lewis 8- by 6-foot supersonic tunnel at Mach numbers of 1.6, 1.8, and 2.0 at angles of attack from 0° to 9°. The inlet was designed to attain a mass-flow ratio of unity at a flight Mach number of 2.0. The two bypasses were about 6 inlet diameters downstream of the inlet entrance and each was designed to discharge in a nearly axial direction about 10 percent of the maximum capture mass flow of the inlet. A closed position of the bypass was also tested. Force and pressure-recovery data were obtained and are presented without detailed analysis.

At a flight Mach number of 2.0 and with a full free-stream tube entering the inlet, the increase in drag associated with bypassing about 23 percent of the stream tube was only one-fifth of the additive drag that would result if the same amount of air were spilled behind an inlet normal shock. At flight Mach numbers of 1.8 and 1.6, the increases in drag were one-fourth and one-tenth, respectively, of the additive drag associated with equivalent normal-shock spillage. The open or closed position of the bypass did not significantly reduce the diffuser pressure recovery as compared with the inlet performance obtained without bypasses. The bypass mass-flow ratio was practically constant in the region of subcritical inlet flow, but varied for supercritical inlet flow at each angle of attack and flight Mach number. For the range of angles of attack investigated, the lift coefficients were higher than those obtained without bypasses.

INTRODUCTION

During certain phases of the flight path of a supersonic aircraft, the mass-flow capacity of a fixed-geometry inlet may exceed that required

[redacted]

[redacted]

by the engine and result in subcritical inlet operation and attendent high drags (references 1 and 2). Several variable-inlet-geometry systems have been proposed to reduce the high drags that result from the spillage of excess mass flow behind an inlet-shock system. Another system, generally referred to as a bypass, permits the inlet to operate at critical flow (minimum drag and high pressure recovery) by discharging excess mass flow through a scoop or bypass located in the subsonic diffuser forward of the engine. The merit of the bypass system depends on the relative performance penalties associated with the bypassed air compared with the additive drag which results from spilling air behind an inlet normal shock.

As part of a general program to provide design data on the force and pressure-recovery characteristics of variable-air-flow supersonic inlets, an axially symmetric spike-type inlet suitable for a nacelle power-plant installation with two fixed-area bypasses located in a horizontal plane and on opposite sides of the subsonic diffuser has been investigated in the NACA Lewis 8- by 6-foot supersonic tunnel. The inlet was designed to attain a mass-flow ratio of unity at a flight Mach number of 2.0. Each of the fixed-area bypasses was designed to discharge approximately 10 percent of the mass flow captured by the inlet. Tests were also made with the lip of the bypass in a closed or no-flow position.

Aerodynamic and pressure-recovery characteristics of the configuration with open and closed bypasses are presented without detailed analysis for a range of mass-flow ratios at flight Mach numbers of 1.6, 1.8, and 2.0 at angles of attack up to 9°.

SYMBOLS

The following symbols are used in this report:

A	area
A_m	external maximum cross-sectional area
a/a_a	ratio of local to stagnation sonic velocities
C_D	drag coefficient, external drag plus internal and external drag due to bypassing mass flow, D/q_0A_m
C_L	lift coefficient, measured lift minus internal lift due to engine mass flow/q_0A_m
$C_{L,e}$	external-lift coefficient, $\frac{\text{external lift}}{q_0A_m}$

C_M pitching-moment coefficient about base of model, total minus internal pitching moment due to engine mass flow/$q_0 A_m l$

C_{T-D} thrust-minus-drag coefficient, $\frac{T - D}{q_0 A_m}$

D drag force

L length of subsonic diffuser, 46.9 in.

l over-all length of model, 58.7 in.

M Mach number

m mass flow

m_4/m_0 engine mass-flow ratio, $\frac{\text{engine mass flow}}{\rho_0 V_0 A_1}$

m_b/m_0 bypass mass-flow ratio, $\frac{\text{bypass mass flow}}{\rho_0 V_0 A_1}$

P total pressure

p static pressure

q dynamic pressure, $\gamma p M^2/2$

T thrust, net force in flight direction due to change of momentum of engine mass flow between free stream (station 0) and diffuser discharge (station 4) including force on base of balance

V velocity

x longitudinal station, in.

α nominal angle of attack, deg

γ ratio of specific heats for air

ρ mass density of air

Subscripts:

b bypass

x longitudinal station

0 free stream

1 leading edge of cowl

4 diffuser discharge at constant diameter section, station 46.9

4,1 diffuser discharge at constant diameter section (sting out), station 46.9

Pertinent areas:

A_m external maximum cross-sectional area, 0.360 sq ft

A_1 inlet capture area defined by cowl lip (measured), 0.155 sq ft

A_4 flow area at diffuser discharge, 0.289 sq ft

$A_{4,1}$ flow area at diffuser discharge (sting out), 0.338 sq ft

APPARATUS AND PROCEDURE

The configuration investigated, shown schematically in figure 1, consisted of a single-conical-shock inlet without internal contraction, an annular subsonic diffuser, and two fixed-area bypasses located in a horizontal plane on opposite sides of the body. Tip projection of the 25° half-cone was selected so that the conical shock would be tangent to the cowl lip at a flight Mach number of 2.0. The external slope of the cowl lip was nearly alined with the local streamline behind the oblique shock. Coordinates of the cowl and centerbody are presented in table I. The leading edges of the two bypasses were approximately 6 inlet diameters downstream of the inlet entrance and slightly forward of the engine or combustion chamber. With the exception of the bypass inserts, the configuration is the same as inlet B of reference 3.

Photographs of the open and closed bypass inserts are shown in figure 2 and typical cross sections, details, and coordinates are shown in figure 3. The minimum area of the nozzle was sized to permit discharge of approximately 10 percent of the maximum mass flow captured by the inlet at an estimated peak inlet pressure recovery. The flow passage between the outer body and the bypass insert was a convergent-divergent asymmetric nozzle; the external surface of the bypass formed a channel with a discharge angle of $3\frac{1}{2}^\circ$ relative to the model center line. The bypass insert did not protrude beyond the external surface of the model. The closed bypass configuration (fig. 2(d) and dashed lines in fig. 3) represents the no-flow position of one possible type of variable-mass-flow bypass and was tested to determine the installation penalty. The longitudinal area variation of the subsonic diffuser, shown in figure 4 for the open and closed bypasses, is the ratio of the local flow area based on the average normal to the annulus surfaces and the maximum flow area at the diffuser discharge, station 46.9.

The model was sting mounted from the tunnel strut. Forces were measured by an internal three-component strain-gage balance. The pressure acting on the base of the balance was measured by means of a static tube. Angles of attack were determined by using balance normal and moment readings in conjunction with a static calibration of model and sting deflections. Regions of inlet instability or pulsing were determined from time-force histories of net axial-force variations and high-speed schlieren photographs.

The amount of mass flow available to the engine and the amount bypassed are presented as ratios based on the mass flow of a free-stream tube defined by the cowling capture area. The sum of the two ratios is the mass-flow ratio of the inlet. The engine mass-flow ratio was computed at the plane of survey (station 36.7) using the average of eight static-pressure tubes (the maximum deviation of the static-pressure tubes was less than 1 percent) and the Mach number determined by applying the isentropic one-dimensional area-ratio relation between the plane of survey and the sonic discharge area which was assumed to be the minimum geometric area at the control plug measured normal to the outerbody.

The method of instrumentation and the assumptions made for the calculation result in an over-estimation of the mass-flow ratio of not more than 2 percent at zero angle of attack and of about 3 percent at the adverse condition of an angle of attack of 9°. A similar method was used in reference 3, but because the bypass inserts were not installed, the error in mass flow was less than 1 percent. Total-pressure recoveries were computed from the average static pressure and the Mach number at the plane of survey.

The thrust-minus-drag coefficients presented include the force on the base of the strain-gage balance and are approximately equivalent to the net force on the model with the mounting sting removed. Accordingly, the diffuser-discharge Mach numbers and force and pressure-recovery performance data were referred to the maximum constant-area section of the diffuser (station 46.9) from the plane of survey with the flow area (at station 46.9) increased by an amount equivalent to the cross-sectional area of the support sting by appling isentropic one-dimensional flow relations.

The bypass mass-flow ratio was computed from the relation

$$\frac{m_b}{m_0} = \frac{p_b A_b M_b (a/a_a)_0}{p_0 A_1 M_0 (a/a_a)_b}$$

where the static pressure p_b in the subsonic portion of the bypass nozzle and the free-stream conditions were known. The quantity $A_b M_b/(a/a_a)_b$ was evaluated from the bypass mass-flow ratio for supercritical engine inlet flow which was established as the difference between supercritical mass-flow ratios of the inlet without and with bypasses;

the quantity $A_b M_b/(a/a_a)_b$ was assumed to be constant for computation of the bypass mass flow for subcritical inlet flow. (Since the subsonic contraction ratio of the bypass was constant and the throat of the bypass was always choked, the Mach number at the measuring station should remain constant if changes in the effective area due to varying mass flow are small. Additional calculations of the bypass mass flows employing the static pressure p_b and the bypass Mach number M_b, determined from the design-area ratio $\frac{A_b}{\text{bypass choked area}}$, substantiate the preceding assumption.)

The sum of the engine and bypass mass-flow ratios at critical inlet flow will not in all cases agree with the critical inlet mass-flow ratios obtained without bypasses (reference 3) because of the difficulty of accurately establishing the point of critical inlet flow and because of the previously discussed computational errors.

The Reynolds number, based on inlet diameter, varied from 2.06 to 2.24×10^6.

RESULTS

The variation of bypass mass-flow ratio, total-pressure recovery, diffuser-discharge Mach number, thrust-minus-drag coefficient, and drag coefficient with engine mass-flow ratio for flight Mach numbers of 1.6, 1.8, and 2.0 are presented in figures 5 and 9 for a nominal angle of attack of zero and in figures 6 and 10 for a nominal angle of attack of 6° for the inlet with open and closed bypasses, respectively. Similar data for nominal angles of attack of 3° and 9° at a flight Mach number of 2.0 are presented in figures 7 and 11. Lift and pitching-moment coefficients for all flight Mach numbers and angles of attack investigated are presented in figures 8 and 12. The actual angles of attack were as much as 0.4° greater than the nominal angles of attack; however, all data have been reduced for the nominal angles of attack.

The thrust-minus-drag coefficients were obtained from the strain-gage balance readings and correspond to the net force on the model in the flight direction (sting removed). This coefficient is an aid in general comparisons of data. Furthermore, this coefficient can be used directly in computing inlet-engine performance since the over-all thrust of the propulsive unit is comprised of the net forces of the inlet-diffuser, engine, and exit nozzle. The thrust is defined as the force developed by the change in momentum of the mass flow delivered to the engine between the free stream and the diffuser discharge. The drag force, obtained by subtracting the measured thrust minus drag from the computed thrust, thus includes the external drag of the model plus the net internal and external effect due to bypassing mass flow. Similarly, the lift and pitching-moment coefficients are the difference between the measured and the computed value of the internal lift or pitching moment caused by the engine mass flow. The additive components due to mass-flow

spillage behind the inlet-shock system are included in the drag, lift, and pitching-moment coefficients. The computed pitching-moment coefficients assume that the turning of the engine mass flow occurred at the cowl lip.

DISCUSSION

Performance with Open Bypasses

The diffuser total-pressure recovery was not significantly affected by discharging mass flow by means of the bypasses. For critical inlet flow at a flight Mach number of 2.0 and zero angle of attack, a total-pressure recovery of 0.83 was attained for the model with open bypasses as compared with 0.84 for the model without bypasses; at a flight Mach number of 1.6 the pressure recovery was reduced from 0.92 to 0.91 by the addition of bypasses (fig. 5(a)). Since the bypass nozzle was always choked, the mass flow bypassed depends on the area and total pressure at the sonic point. The total pressure at the sonic point is not necessarily the same as that at the diffuser discharge but depends on the profile of the flow or content of the internal stream tube captured by the bypass as well as the influence of the bypass on the profile. For the subcritical inlet flow region, the bypass mass flow remained relatively constant. This indicates that the bypass total pressure did not change which can be associated with the fairly constant diffuser total-pressure recovery for subcritical flow attained with the particular configuration investigated. As a result of constant bypass mass flow for subcritical flow, the mass flow available to the engine was correspondingly reduced. In the region of supercritical (constant) inlet flow, the bypass mass-flow ratio is not constant since there is a progressive reduction in total-pressure recovery due to the normal-shock movement in the diffuser. This effect produces a variable engine mass-flow ratio in the supercritical inlet flow region. However, the performance at conditions other than critical inlet flow is of secondary importance because an actual application of the bypass system would probably utilize a bypass with a variable minimum area in order to maintain critical inlet flow conditions over a range of engine mass-flow requirements.

At the design point of the bypass (critical inlet flow, $M_0 = 2.0$, $\alpha = 0$), the drag coefficient of the model was increased about 20 percent as a result of internal and external drag attributed to bypassing 23 percent of the maximum capture mass flow, which is only one-fifth of the additive drag that would result by spilling the same amount of air behind the inlet normal shock (fig. 5(b)). At a flight Mach number of 1.8, the increase in drag due to bypassing was about one-fourth of the corresponding additive drag associated with normal-shock spillage and about one-tenth at a flight Mach number of 1.6. Comparing the thrust-minus-drag coefficients (thus considering the net effects of drag and pressure recovery) shows that maintaining critical inlet-flow conditions and discharging excess mass flow by means of a bypass increased the net force on the model in the flight direction approximately 12 percent

at a flight Mach number of 2.0 when compared with inlet-shock spillage at an equivalent engine mass-flow ratio (fig. 5(b)).

The lift coefficients shown in figure 8 are generally higher over the range of mass-flow ratios and angles of attack than those obtained without bypasses. For a flight Mach number of 2.0 and critical inlet flow, the lift increased about 33 percent for an angle of attack of 3°. At angles of attack of 6° and 9°, the lift increases were approximately 14 and 20 percent, respectively. This increase is the result of internal and external effects of the bypassed mass flow. Externally the bypass jet and the body cross flow mix and probably alter the external pressure distribution of the body.

When comparison is made at the same engine mass-flow ratios, for example at an angle of attack of 3°, a higher lift is obtained by discharging mass flow through the bypasses. This can also be attributed to the internal lift due to bypassing, whereas no internal lift is included in the coefficient obtained in reference 3 with inlet-normal shock spillage.

Performance with Closed Bypasses

The error in mass-flow ratio discussed in the APPARATUS AND PROCEDURE section is apparent in the data obtained with the bypasses closed (figs. 9 to 11), where increases in mass-flow ratio are indicated for supercritical inlet flow. Inasmuch as inlet conditions were not changed by the closed bypasses, the critical mass-flow ratios have been faired to agree with the results obtained without bypass inserts (reference 3).

The total-pressure recoveries (at the same longitudinal measuring station but not at equal flow areas) were not significantly altered by the addition of closed bypass inserts compared with the results obtained in reference 3. The minimum drag coefficients were increased about 16 percent at a flight Mach number of 2.0 and 20 percent at a flight Mach number of 1.6 (fig. 9(b)). This is primarily attributed to the base drag on the external surface of the closed lip of the bypasses and could probably be reduced by modifying the design.

The cross flow at angle of attack over the external surface of the bypass insert had a negligible effect on the lift coefficient.

SUMMARY OF RESULTS

The following results were obtained from an investigation of the force and pressure-recovery characteristics of a nacelle-type conical spike inlet model with two fixed-area bypasses.

2759

1. For critical inlet flow at a flight Mach number of 2.0, the increase in drag for bypassing about 23 percent of the maximum capture mass flow of the inlet was only one-fifth of the additive drag that would result if the same amount of air were spilled behind an inlet normal shock. At a flight Mach number of 1.8 the drag due to bypassing was about one-fourth of the additive drag for equivalent normal-shock spillage and about one-tenth at a flight Mach number of 1.6.

2. The diffuser total-pressure recovery was not significantly reduced when air was bypassed or when the lips of the bypass were closed as compared with results obtained without bypasses.

3. The lift coefficients were higher over the range of angles of attack investigated than those obtained without bypasses.

4. The bypass system discharged a nearly constant mass flow for subcritical inlet flow at each flight Mach number and angle of attack investigated.

Lewis Flight Propulsion Laboratory
National Advisory Committee for Aeronautics
Cleveland, Ohio

REFERENCES

1. Schueller, Carl F., and Esenwein, Fred T.: Analytical and Experimental Investigation of Inlet-Engine Matching for Turbojet-Powered Aircraft at Mach Numbers up to 2.0. NACA RM E51K20, 1952.

2. Blackaby, James R.: An Analytical Study of the Comparative Performance of Four Air-Induction Systems for Turbojet-Powered Airplanes Designed to Operate at Mach Numbers up to 1.5. NACA RM A52C14, 1952.

3. Beke, Andrew, and Allen J. L.: Force and Pressure Recovery Characteristics of a Conical-Type Nose Inlet Operating at Mach Numbers of 1.6 to 2.0 and at Angles of Attack to 9°. NACA RM E52I30, 1952.

TABLE I. - COORDINATES

(a) Centerbody

Station (in.)	Radius (in.)
-2.86	[a]0
- .2	[a]1.24
.0	1.32
.1	1.36
.2	1.39
.3	1.42
.4	1.45
.5	1.48
.8	1.56
1.0	1.61
1.5	1.73
2.0	1.84
2.5	1.92
3.0	2.01
4.0	2.14
5.0	2.24
6.0	2.31
7.0	2.37
8.0	2.42
9.0	2.44
10.0	2.46
12.0	2.46
14.0	2.44
16.0	2.40
18.0	2.32
20.0	2.19
22.4	2.03
24.0	1.95
28.0	1.75
32.0	1.61
37.1	1.50
46.9	1.50

(b) Cowling

Station (in.)	External radius (in.)	Internal radius (in.)
0.0	2.671	2.671
.015	2.686	2.656
.5	2.79	2.73
1.0	2.89	2.80
1.5	2.97	2.86
2.0	3.04	2.92
2.5	3.11	2.98
3.0	3.16	3.03
4.0	3.25	3.12
5.0	3.32	3.20
6.0	3.38	3.25
7.0	3.42	3.30
8.0	3.45	3.33
8.67	3.47	3.35

[a]Region of 25°-half-angle cone.

[redacted]

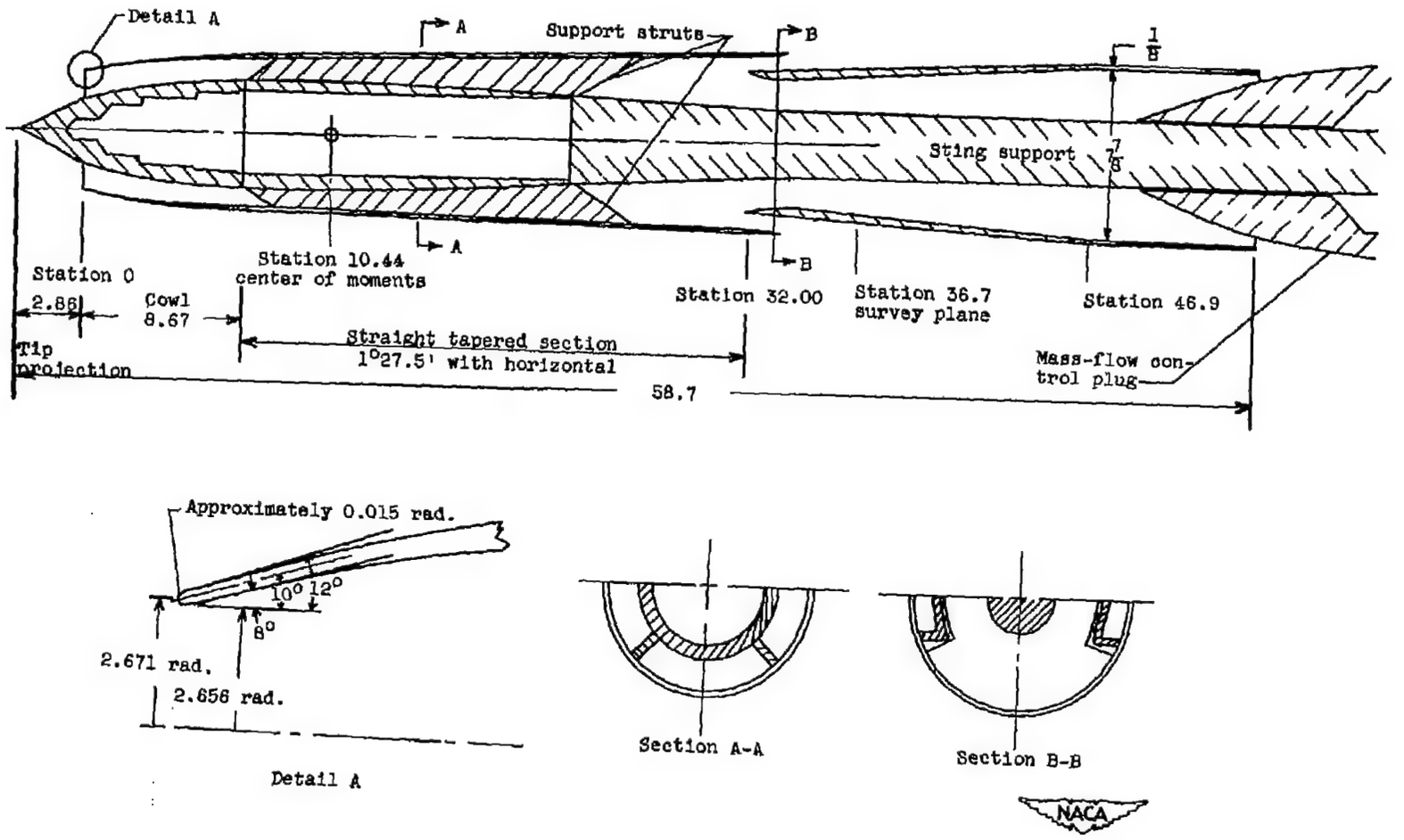

Figure 1. - Schematic diagram of plan form of model. (All dimensions in inches.)

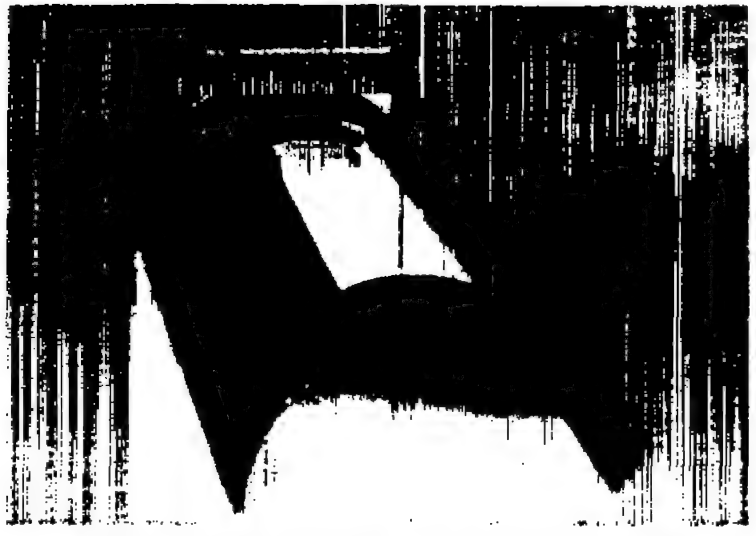

(a) External view of open bypass (looking forward).

(b) Internal view of open bypass (looking aft).

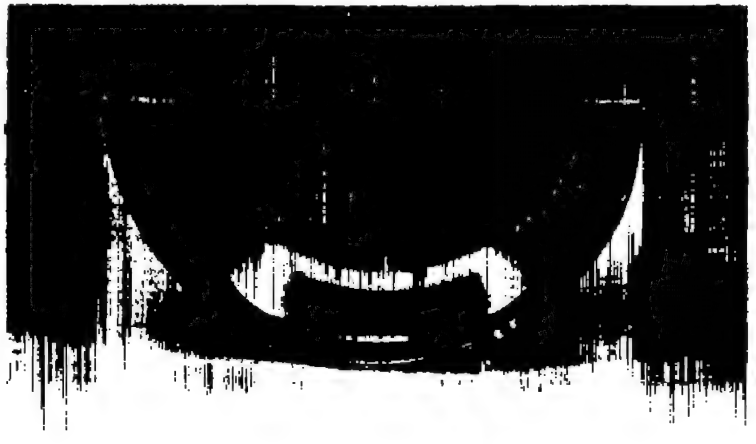

(c) Front view of open bypass (looking aft).

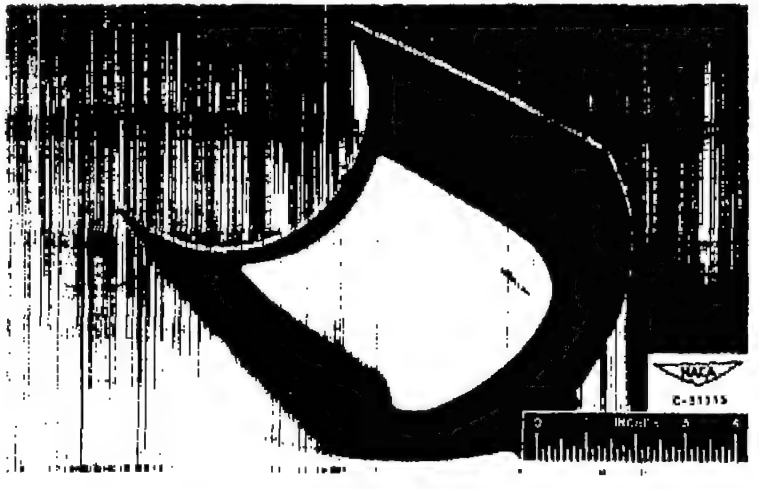

(d) Internal view of closed bypass (looking aft).

Figure 2. - Photographs of bypass.

x	y	z	Flow area
0	0.94	3.63	3.50
.2	.788	3.30	2.62
.4	.712	3.18	2.40
.6	.680	3.08	2.22
.8	.627	3.02	2.03
.9	.618	3.02	1.90
1.0	.604	3.02	1.82
1.25	.650	3.02	1.97
1.64	.700	3.02	2.07

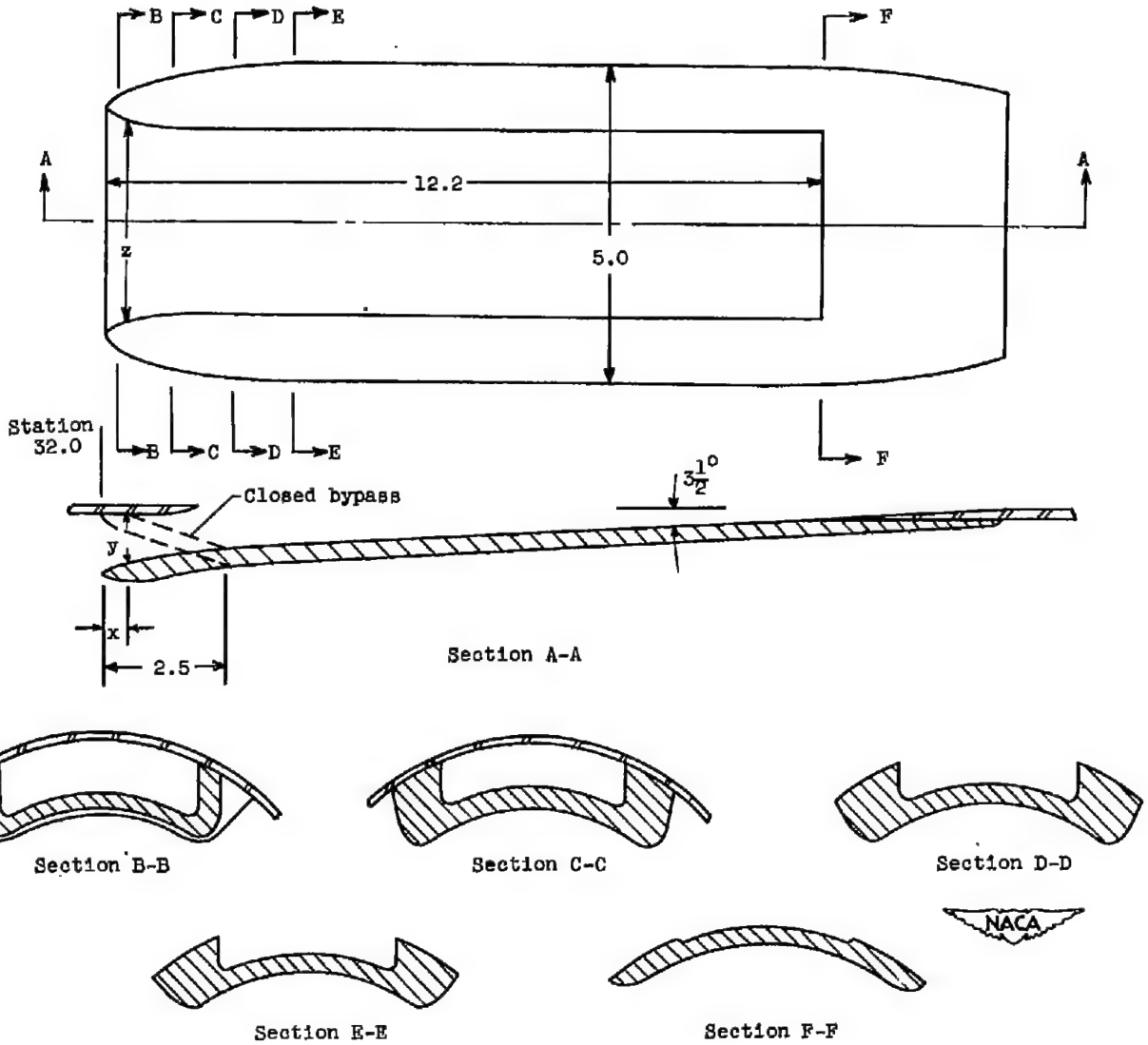

Figure 3. - Details of axial-discharge bypass. (All dimensions in inches.)

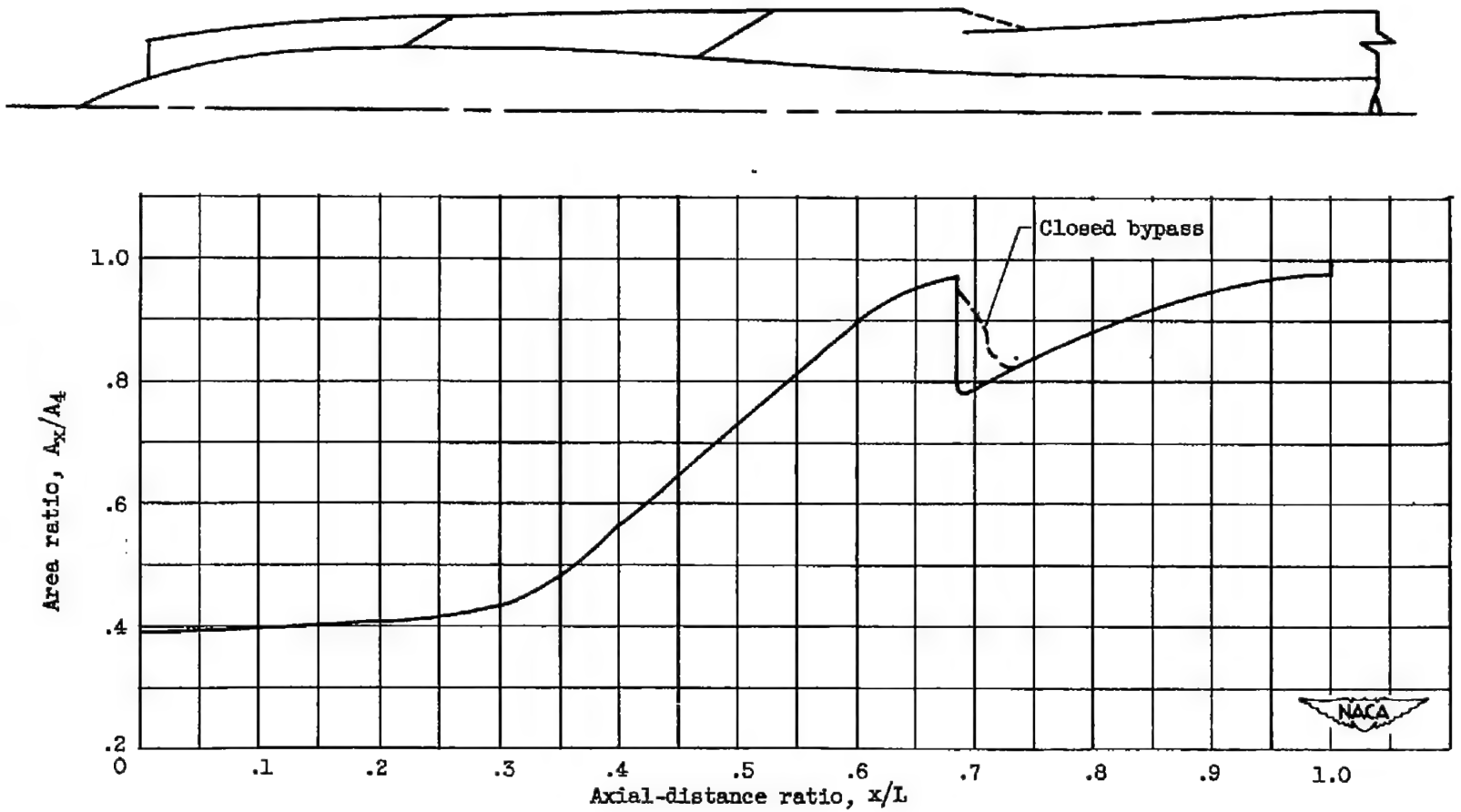

Figure 4. - Subsonic-diffuser area variation.

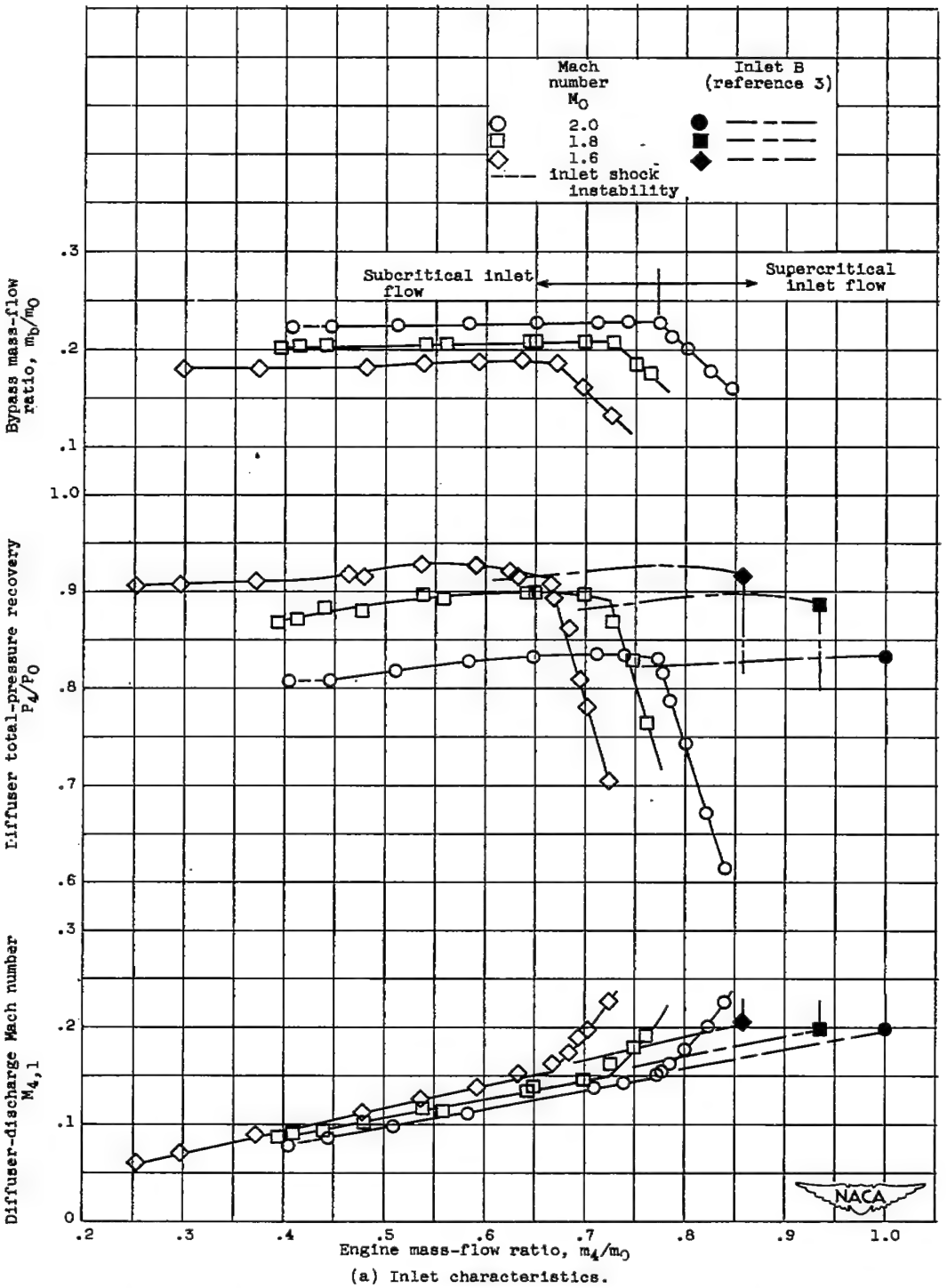

(a) Inlet characteristics.

Figure 5. - Variation of inlet characteristics and force coefficients with mass-flow ratio for a range of Mach numbers. Model with bypasses open; zero angle of attack.

[redacted]

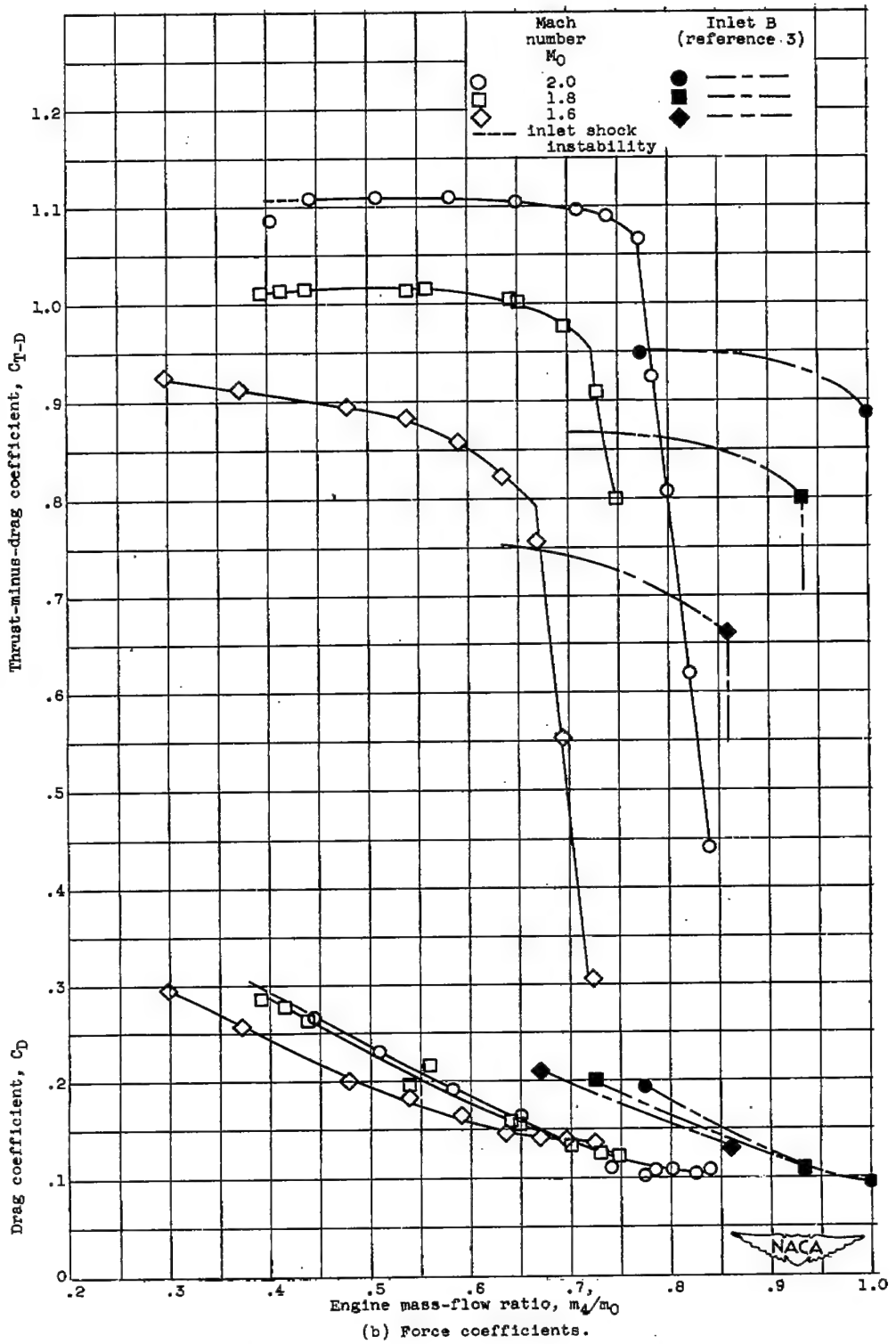

(b) Force coefficients.

Figure 5. - Concluded. Variation of inlet characteristics and force coefficients with mass-flow ratio for a range of Mach numbers. Model with bypasses open; zero angle of attack.

[redacted]

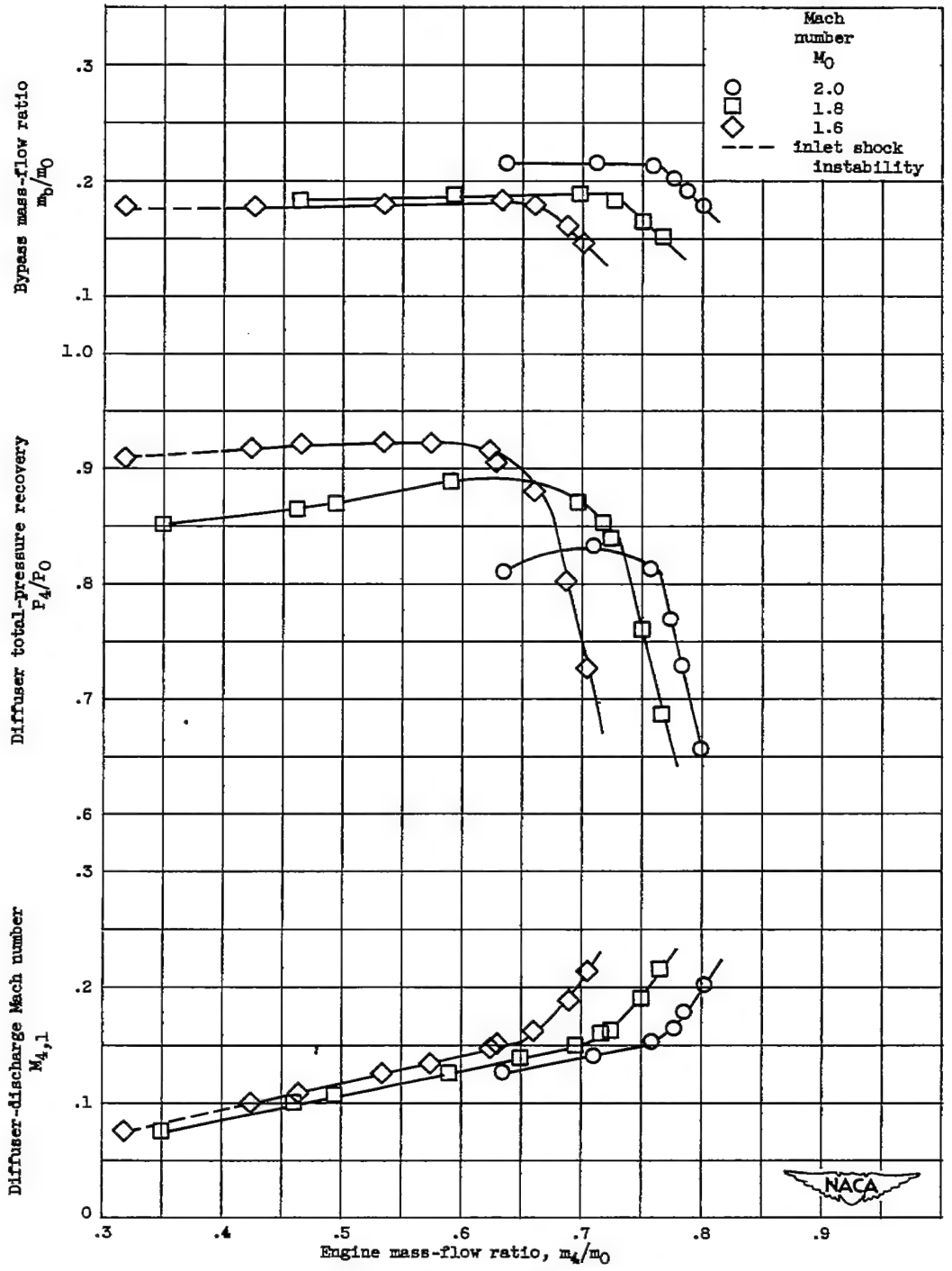

(a) Inlet characteristics.

Figure 6. - Variation of inlet characteristics and force coefficients with mass-flow ratio for a range of Mach numbers. Model with bypasses open; nominal angle of attack, 6°.

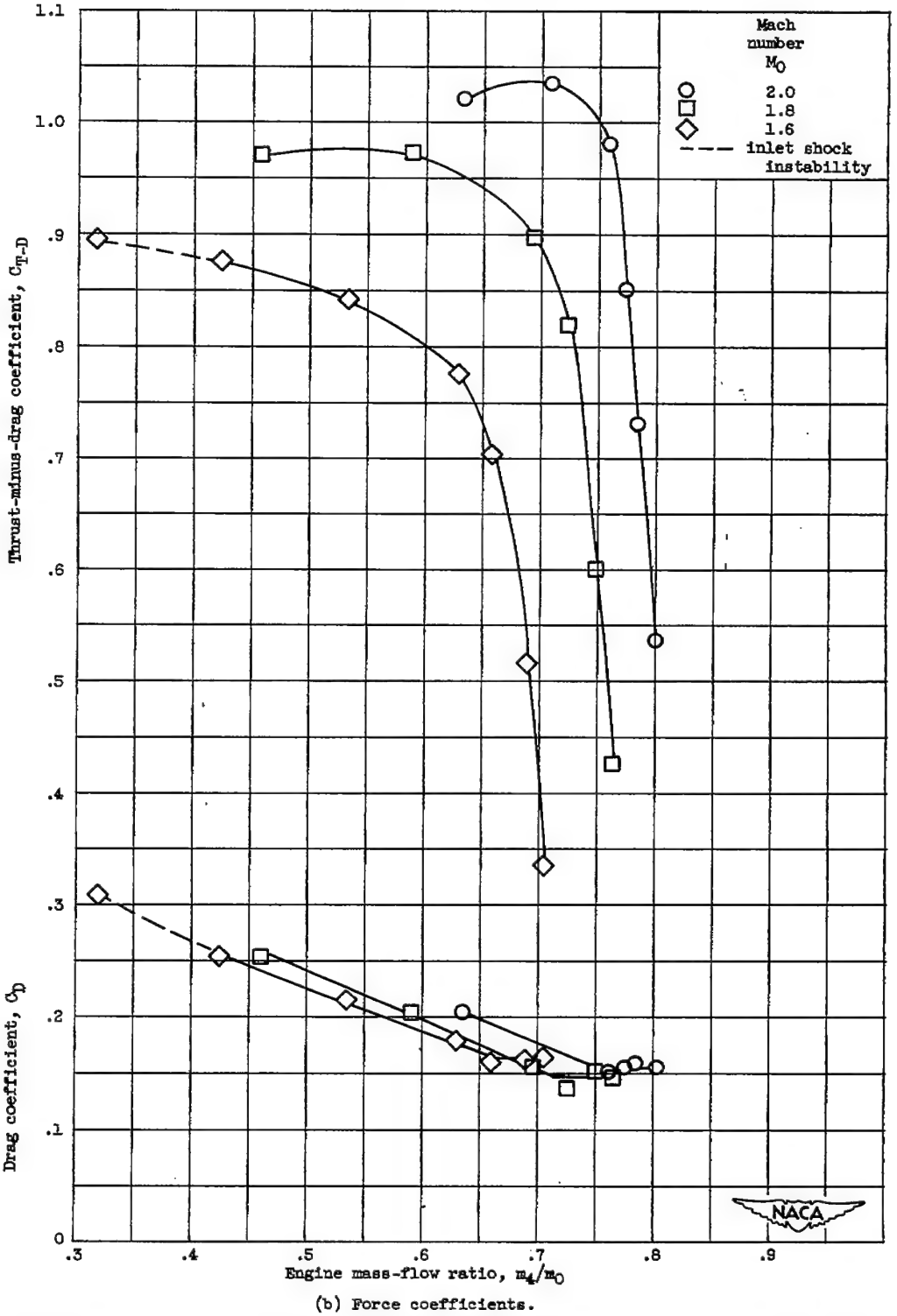

(b) Force coefficients.

Figure 6. - Concluded. Variation of inlet characteristics and force coefficients with mass-flow ratio for a range of Mach numbers. Model with bypasses open; nominal angle of attack, 6°.

[redacted]

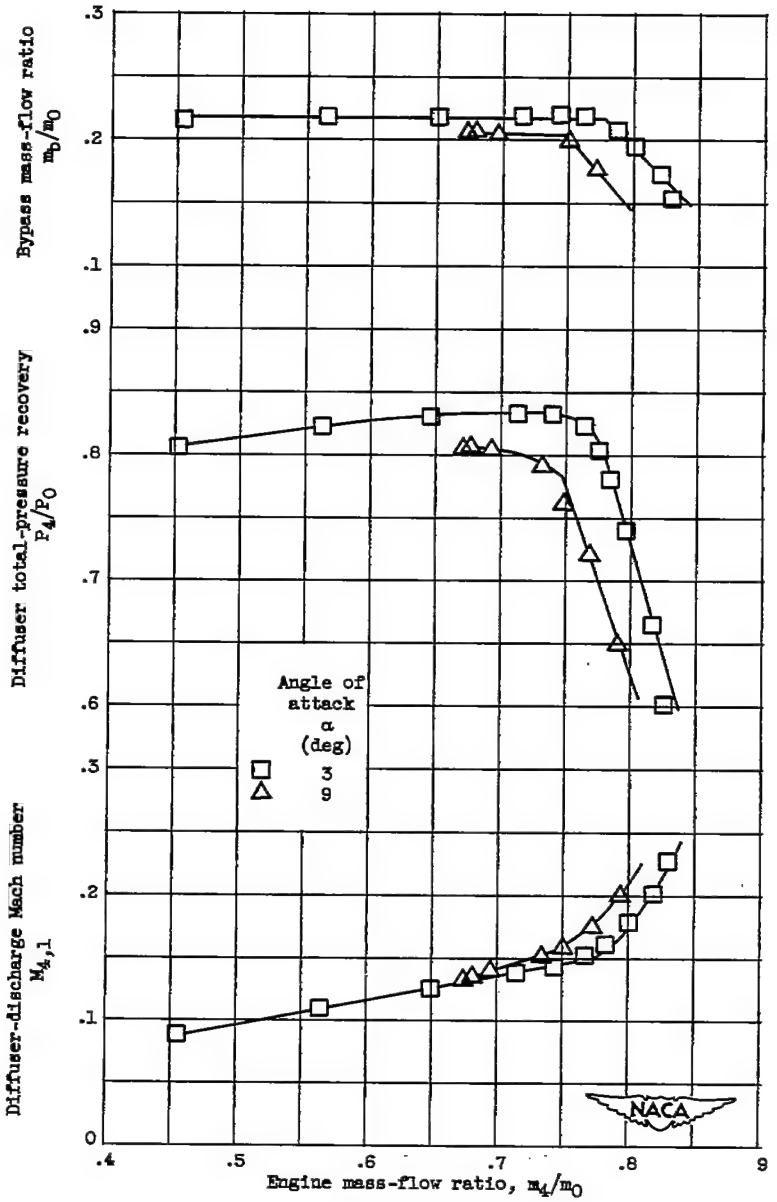

(a) Inlet characteristics.

Figure 7. - Variation of inlet characteristics and force coefficients with mass-flow ratio for a Mach number of 2.0. Model with bypasses open; nominal angle of attack, 3° and 9°.

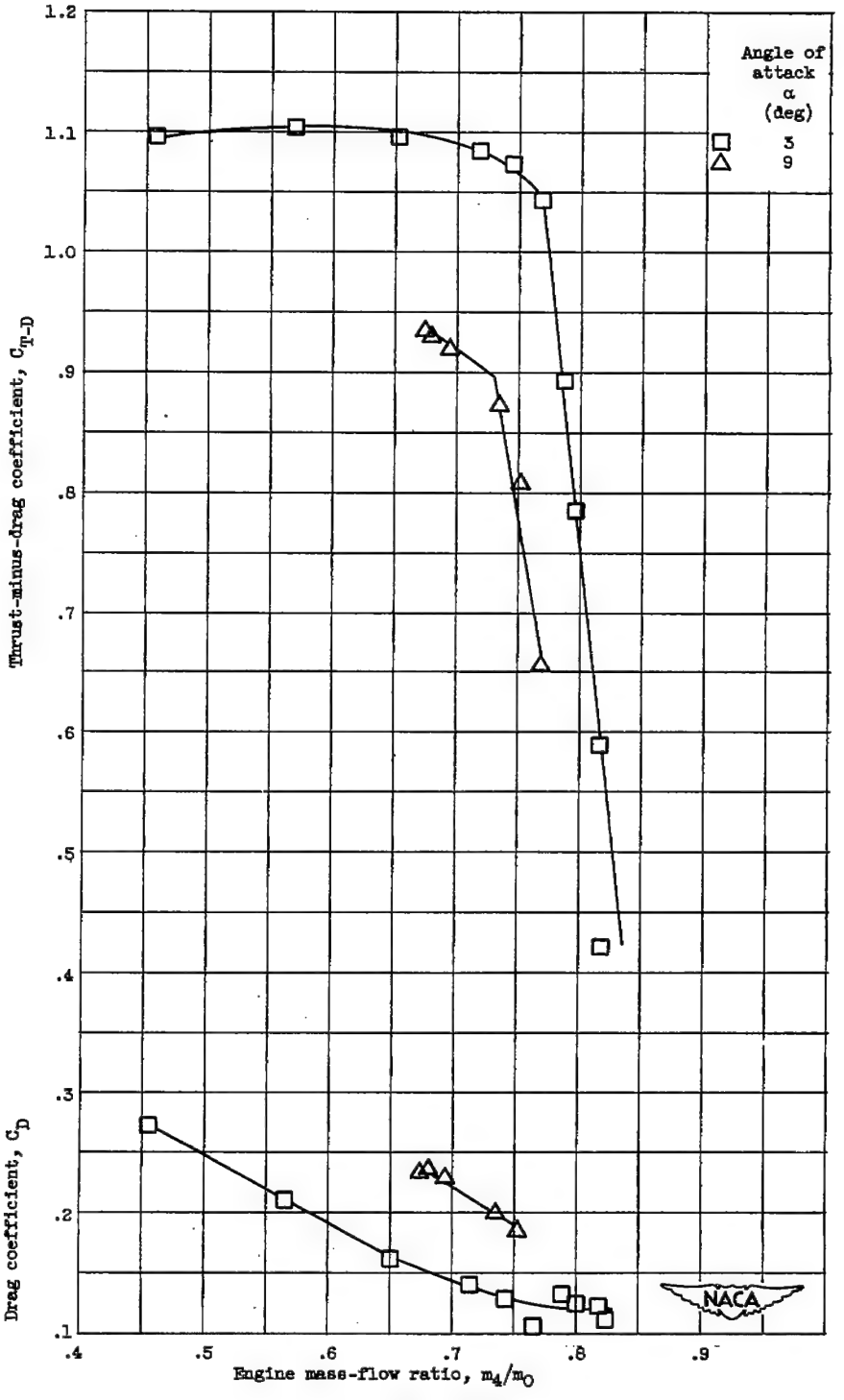

(b) Force coefficients.

Figure 7. - Concluded. Variation of inlet characteristics and force coefficients with mass-flow ratio for a Mach number of 2.0. Model with bypasses open; nominal angle of attack, 3° and 9°.

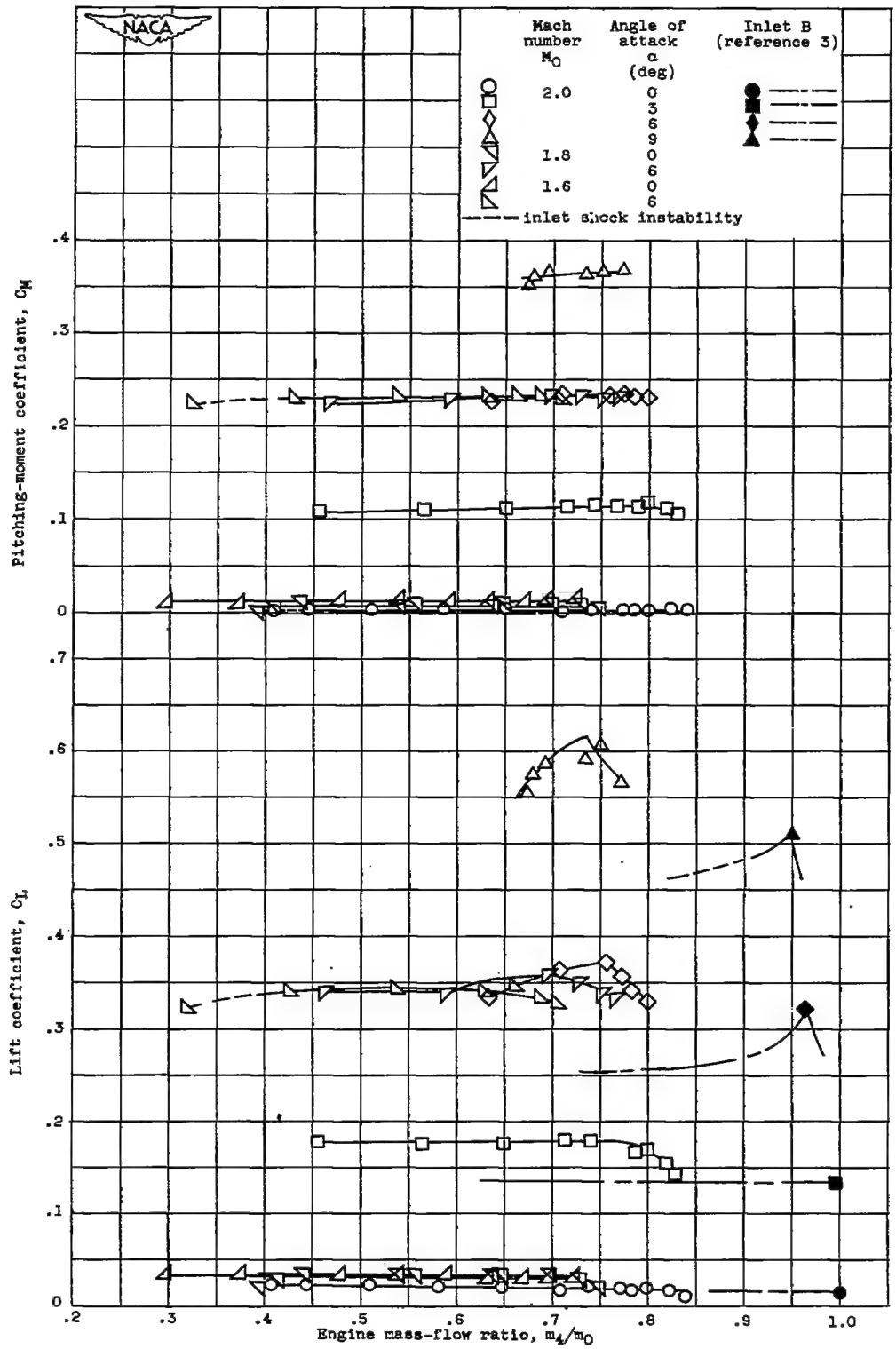

Figure 8. - Variation of lift and pitching-moment coefficients with mass-flow ratio for a range of Mach numbers and nominal angles of attack of 0°, 3°, 6°, and 9°. Model with bypasses open.

[redacted]

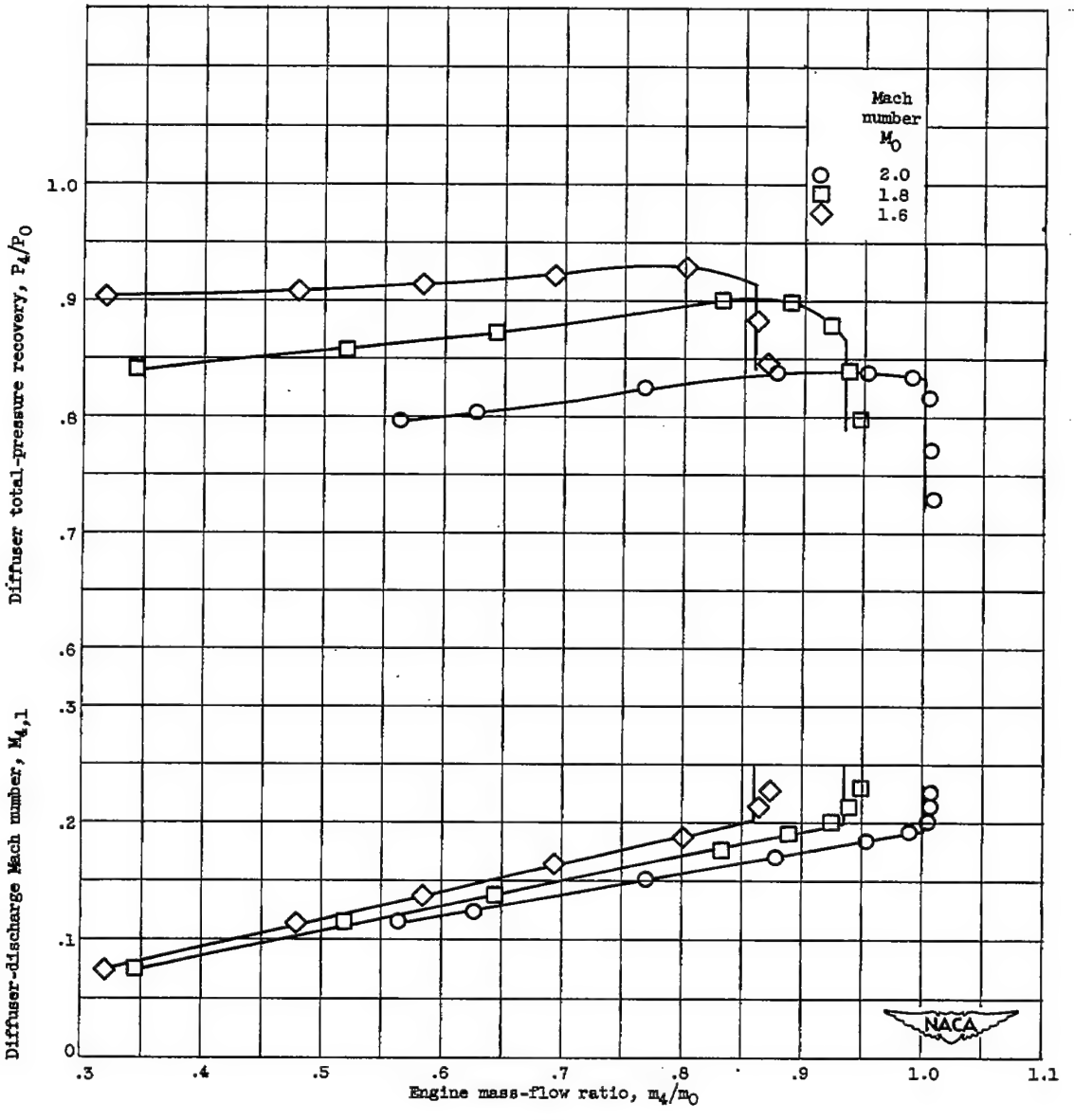

(a) Inlet characteristics.

Figure 9. - Variation of inlet characteristics and force coefficients with mass-flow ratio for a range of Mach numbers. Model with bypasses closed; zero angle of attack.

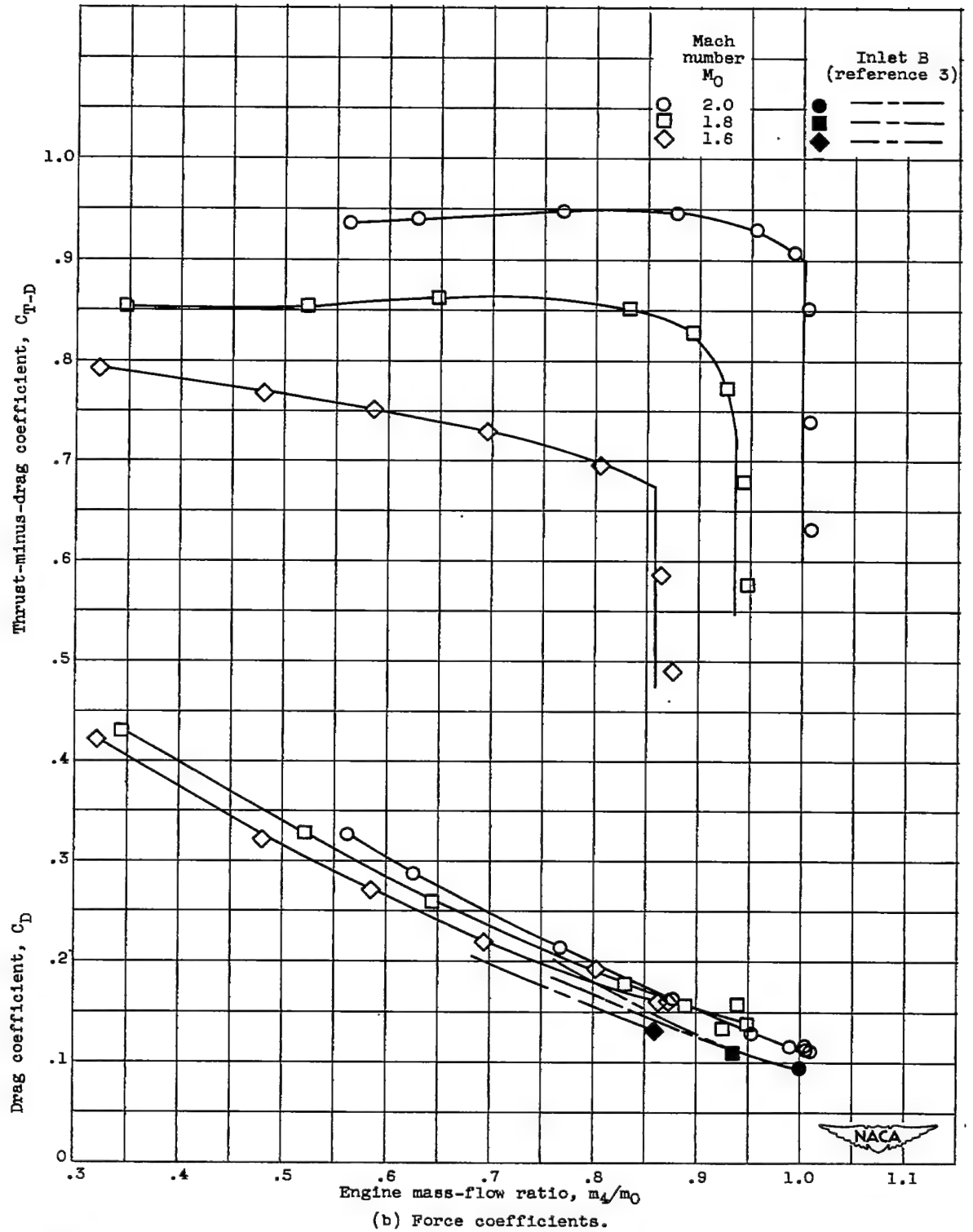

(b) Force coefficients.

Figure 9. - Concluded. Variation of inlet characteristics and force coefficients with mass-flow ratio for a range of Mach numbers. Model with bypasses closed; zero angle of attack.

[redacted]

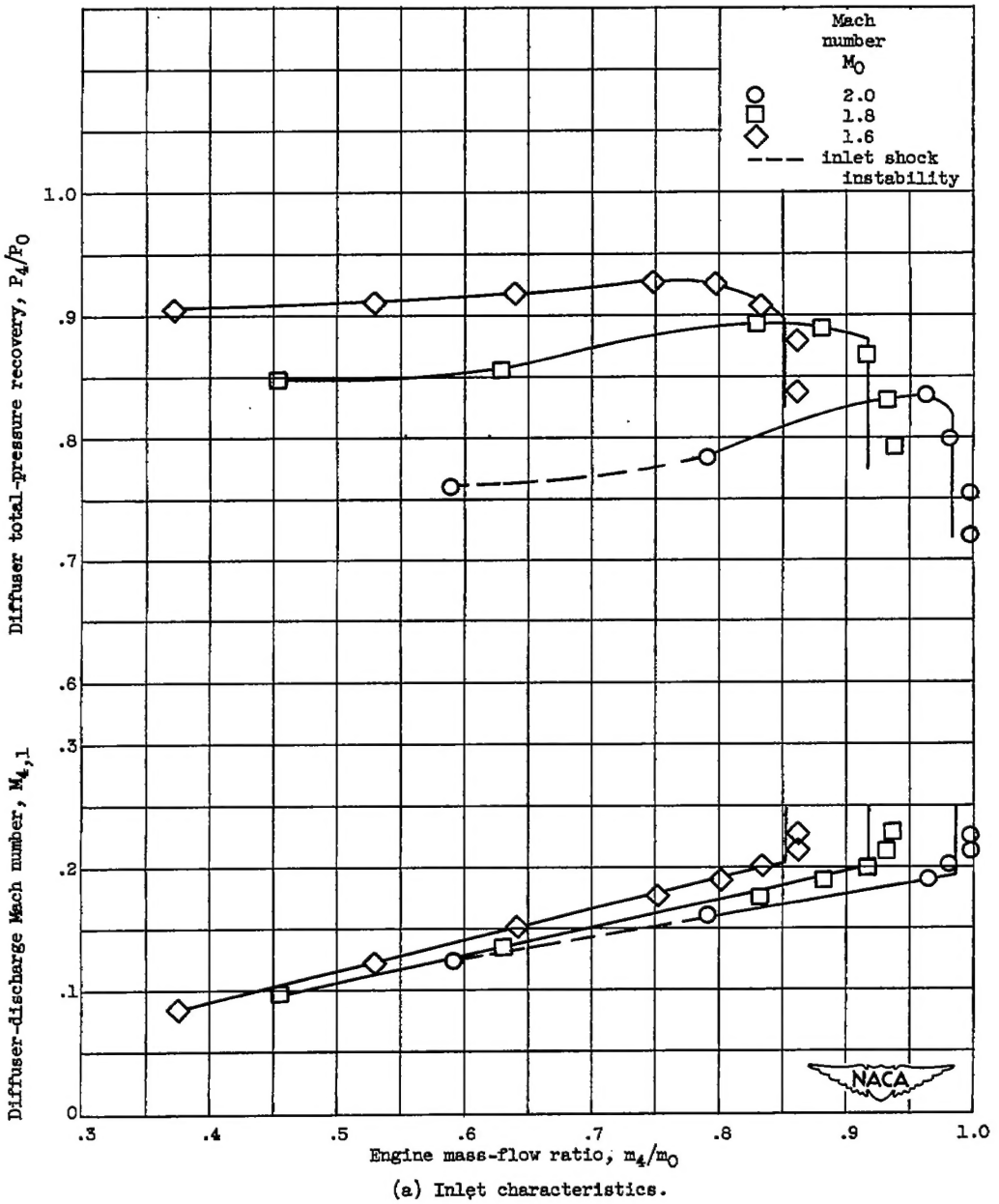

(a) Inlet characteristics.

Figure 10. - Variation of inlet characteristics and force coefficients with mass-flow ratio for a range of Mach numbers. Model with bypasses closed; nominal angle of attack, 6°.

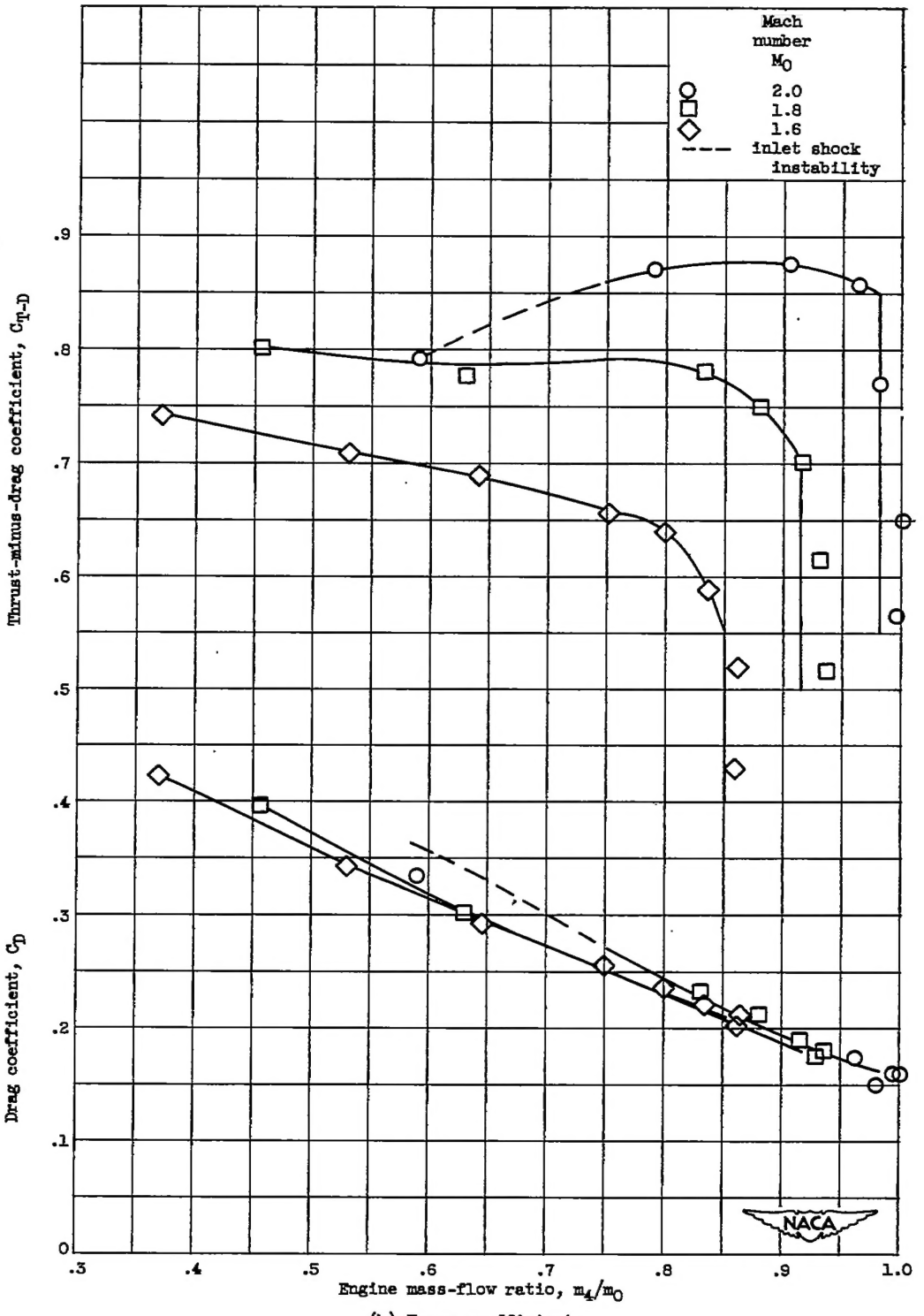

(b) Force coefficients.

Figure 10. - Concluded. Variation of inlet characteristics and force coefficients with mass-flow ratio for a range of Mach numbers. Model with bypasses closed; nominal angle of attack, 6°.

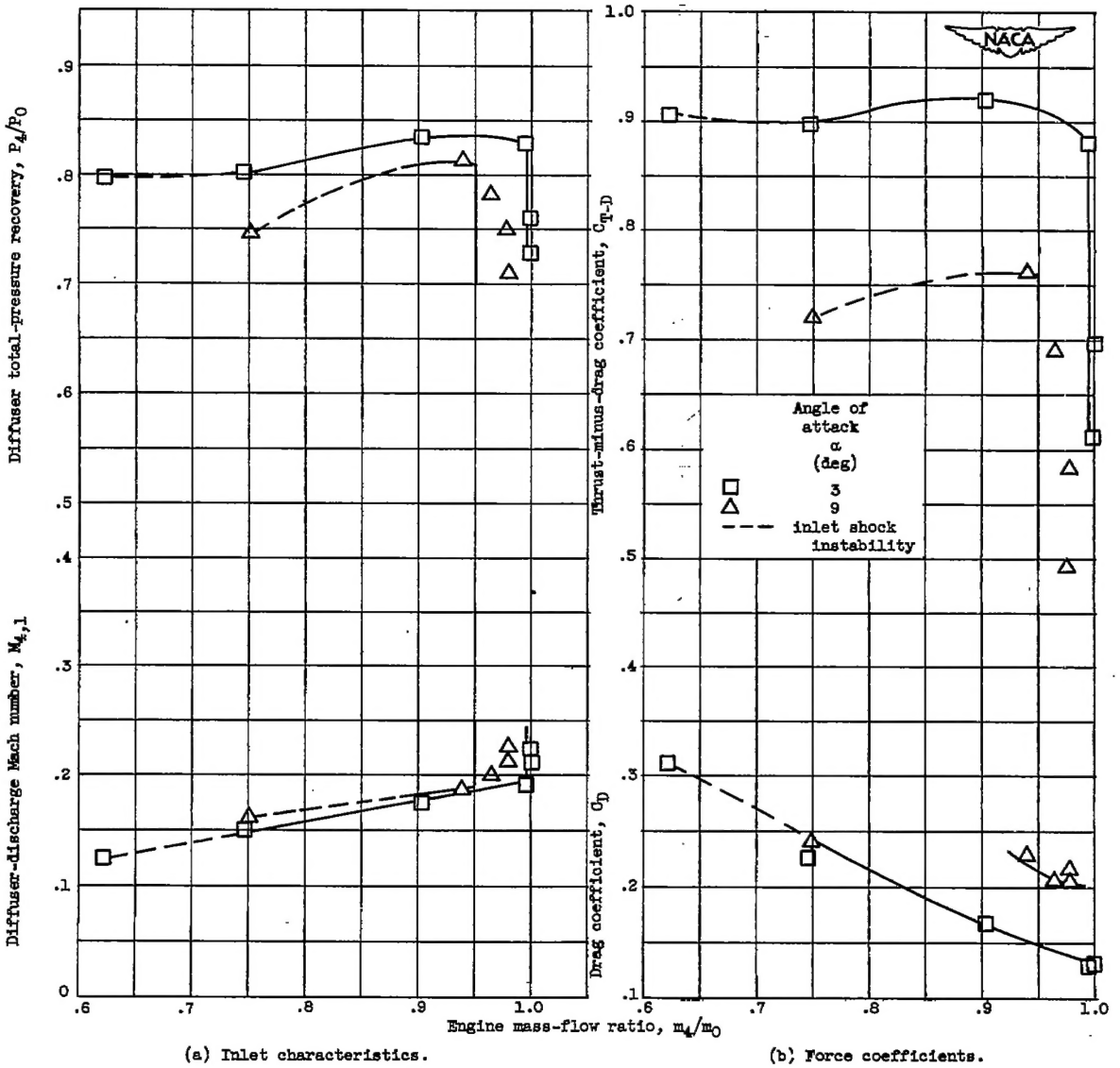

(a) Inlet characteristics. (b) Force coefficients.

Figure 11. - Variation of inlet characteristics and force coefficients with mass-flow ratio for a Mach number of 2.0. Model with bypasses closed; nominal angle of attack, 3° and 9°.

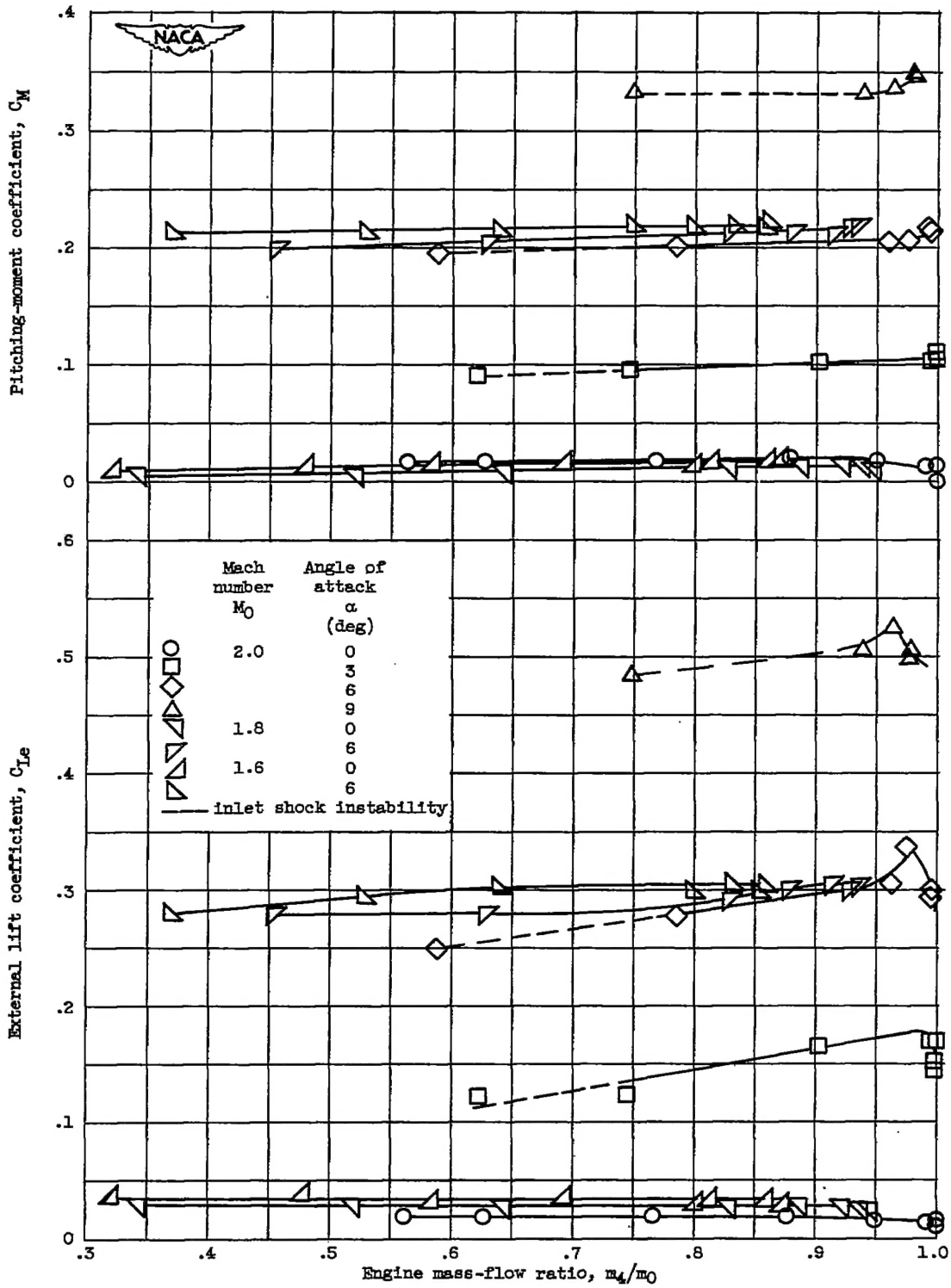

Figure 12. - Variation of lift and pitching-moment coefficients with mass-flow ratio for a range of Mach numbers and nominal angles of attack of 0°, 3°, 6°, and 9°. Model with bypasses closed.

CONFIDENTIAL

NACA-Langley - 1-30-53 - 400